



## Application of harmonic analysis in measuring the corrosion rate of rebar in concrete

R. Vedalakshmi<sup>a,\*</sup>, SP. Manoharan<sup>a</sup>, Ha-Won Song<sup>b</sup>, N. Palaniswamy<sup>a</sup>

<sup>a</sup> Corrosion Protection Division, Central Electrochemical Research Institute, Karaikudi, 630 006, Tamil Nadu, India

<sup>b</sup> School of Civil Engineering, Yonsei University, Seoul 120-749, Republic of Korea

### ARTICLE INFO

#### Article history:

Received 26 November 2008

Accepted 31 July 2009

Available online 9 August 2009

#### Keywords:

A. Steel reinforced concrete

B. EIS

B. Polarization

B. Weight loss

C. Kinetic parameters

### ABSTRACT

The corrosion rate (CR) of rebar embedded in cement mortar, concrete and cement extract is determined using harmonic analysis technique (HA). Simultaneously using other electrochemical techniques such as impedance spectroscopy (EIS) and Tafel extrapolation (TET), the CR was determined and compared with the weight loss method. CR obtained from HA is comparable to that of EIS provided that the Stern–Geary constant ( $B$  value) obtained from HA is used in the calculation. In concrete, comparable corrosion rates are obtained between TET and HA only under active condition of the rebar whereas under passive state, the corrosion current ( $i_{\text{corr}}$ ) by TET is 10 times lower than that of HA. A good agreement is obtained between the HA and weight loss method. The outcome of the result suggests that HA is capable of providing a higher degree of accuracy than that of EIS and TET in the determination of  $i_{\text{corr}}$  in the medium like rebar in concrete having very low rate of corrosion.

© 2009 Elsevier Ltd. All rights reserved.

### 1. Introduction

When assessing the durability of concrete structures, instantaneous corrosion rate measurement of rebar is an important parameter to predict the remaining service life. It is normally obtained using electrochemical techniques such as linear polarization resistance (LPR), electrochemical impedance spectroscopy (EIS), and galvanostatic pulse (GPT) [1–6]. All these electrochemical techniques need Stern–Geary constant ( $B$  value) to calculate the corrosion current ( $i_{\text{corr}}$ ) from the polarization resistance ( $R_p$ ). The  $B$  value derived from the Tafel constants ( $b_a$  and  $b_c$ ) varied from 13 to 52 mV depending upon the corrosive condition of the rebar. Most of the researchers assumed 52 mV for passive and 26 mV for active [7–9].  $B$  was determined by comparing the gravimetric weight loss measurements with the polarization resistance measurements [10,11]. Presumed values can introduce an error by a minimum factor of 2–4 times if the actual  $B$  is substantially different. In durability assessment, the accurate estimation of  $i_{\text{corr}}$  is very important because of the following reasons: (i) to adopt a cost effective strategy during inspection, repairing, strengthening and replacement of corrosion affected concrete structures at appropriate time to prevent premature failure, (ii) to estimate the structural capacity to withstand the extremely aggressive conditions during the remain-

ing service life and (iii) to assess the time to cracking during the propagation period [12]. When predicting the service life of concrete structures, a suitable alternate method is essential to determine the  $i_{\text{corr}}$  precisely. Harmonic analysis is the only electrochemical technique, which has the specific advantage of determining  $i_{\text{corr}}$  directly from the harmonic currents and does not require Tafel constants.

Earlier investigations established that theoretically HA technique is capable of determining  $i_{\text{corr}}$  along with the Tafel slopes from the harmonic currents, allowing for a reliable determination of the corrosion rate [13,14]. Meszaros et al. [15] measured the  $i_{\text{corr}}$  of carbon steel in acid and neutral media using HA technique and inferred that  $i_{\text{corr}}$  determined at 10 mHz was in good agreement with that of impedance method only when the Tafel slopes obtained by the HA method has been used in the Stern–Geary equation. SathyaNarayanan and Balakrishnan [16] studied the iron corrosion in the presence of polyaniline inhibitors in HCl medium using HA and compared with that of TET. The  $i_{\text{corr}}$  obtained from both the methods were found to be agreed well when the frequency of 10 mHz and an amplitude of 5 mV were used. Durnie et al. [17] measured the  $i_{\text{corr}}$  of steel due to CO<sub>2</sub> corrosion in the presence of inhibitors by HA and compared with that of LPR. The studies were conducted at 100 mHz frequency with an ac amplitude of 30 mV and concluded that HA determined Tafel slopes only yielded comparable  $i_{\text{corr}}$  with that of LPR whereas assumed Tafel slopes introduced an error of 100% in the determination of  $i_{\text{corr}}$  by LPR. The results also confirmed the necessity of including third term in the first harmonic current to get reliable corrosion rate by

\* Corresponding author. Address: Corrosion Protection Division, Central Electrochemical Research Institute, Alagappapuram, Karaikudi, 630 006, Tamil Nadu, India. Fax: +91 04565 227779/227713.

E-mail address: [corrveda@yahoo.co.in](mailto:corrveda@yahoo.co.in) (R. Vedalakshmi).

HA. Lawson et al. [18] carried out HA measurement on the rebar embedded in the cement mortar and correlated the  $i_{\text{corr}}$  with that of both LPR and weight loss method. They observed that there is a frequency and amplitude dependency in HA but the frequency values of between 100–150 mHz and 10 mV, respectively, were found to give corrosion rates consistent with the weight loss method and LPR. Dawson et al. [19] measured the  $i_{\text{corr}}$  of prestressing tendons embedded in the beam using HA and found it was inherently more reliable than LPR, as the Stern–Geary constant can be obtained simultaneously. Cramer et al. [20] used the harmonic distortion analysis to find the  $B$  value and corrected the  $i_{\text{corr}}$  measured by the LPR technique. Gowers and Millard [21] arrived at a frequency of 100 mHz which gives a reliable corrosion rate of rebar in concrete using harmonic analysis. Ha-Won Song and Saraswathy [22] and Srinivasan and Saravanan [23] reviewed the advantage of HA over EIS in assessing the corrosion rate of rebar in concrete structures.

The main objective of the present investigation is to validate the reliability of HA technique in assessing the  $i_{\text{corr}}$  of rebar in uncontaminated/chloride contaminated concrete as against EIS and TET after introducing the third term in the first harmonic current. The accuracy of HA in predicting the corrosion rate (CR) was also compared with the weight loss measurement.

## 2. Experimental

### 2.1. Materials

Ordinary Portland cement conforming to IS 8112 [24], equivalent to ASTM Type I cement, was used and the composition was (wt.%)  $\text{SiO}_2$  – 20–21%;  $\text{Al}_2\text{O}_3$  – 5.2–5.6%;  $\text{Fe}_2\text{O}_3$  – 4.2–4.8%;  $\text{CaO}$  – 62–63%;  $\text{MgO}$  – 0.5–0.7%;  $\text{SO}_3$  – 2.4–2.8%; LOI – 1.5–2.5% and others 0.1%. Well-graded river sand and good quality crushed blue granite aggregates conforming to IS 383 [25] were used as fine and coarse aggregates, respectively. Thermomechanically treated bars (TMT) of 10 mm dia was used. Potable water was used for casting the concrete specimens.

### 2.2. Specimen preparation

#### 2.2.1. Studies in cement extract

From 16 mm diameter deformed bar, 10 mm square steel specimen was cut and brazed with 3 mm dia by 150 mm length copper rod. This assembly was encapsulated in epoxy resin leaving an exposed area of 100 mm<sup>2</sup>. Initially, the mill scale was removed by mechanical grinding and polishing with SiC paper starting from 3/0 down to 5/0. Finally the specimen was degreased with trichloroethylene.  $i_{\text{corr}}$  was determined by immersing the steel specimen directly in the cement extract solution. Cement extract was prepared using 100 g of cement with 200 ml of Millipore water. The mixture was thoroughly mixed and shaken vigorously using a microid flask mechanical shaker for 1 h. The extract was collected by filtration. The pH of the extract was 12.80 ± 0.10. The experiment was conducted after 15 min of immersion in the cement extract. The experiment was also conducted in the presence of 1000 ppm of chloride.

#### 2.2.2. Studies on cement mortar

Cylindrical specimens of 50 mm dia × 50 mm height were cast using cement mortar (cement:sand – 1:2 with w/c ratio of 0.5). TMT bars of 10 mm in dia having a length of 25 mm were centrally embedded in the mortar specimen. Both the top and bottom ends were sealed using epoxy compound by leaving an exposed length of 20 mm. Electrical leads were taken and sealed. In one set of specimens, no chloride (0%) was added and in another set of specimens, 1% and 3% sodium chloride by weight of cement was added at the time of casting. Duplicate specimens were cast for each chloride concentration and cured for 28 days in potable water at room temperature. Then the specimens were subjected to an alternate wetting and drying test. 0%, 1% and 3% chloride added cement mortar specimens were kept immersed in 0%, 1% and 3% chloride solution, respectively, for 2 days and dried at 40 °C for 2 days. Thus 4 days constituted one cycle and specimens were subjected to 15 such cycles. Electrochemical measurements were carried out after the completion of the 15th cycle.

#### 2.2.3. Studies on concrete

Two grades of concrete having a compressive strength of 25 and 35 MPa were designed as per the procedure outlined in ACI 211-91 [26]. The details of the mix proportions used are given in Table 1. Cubical concrete specimens having a size of 150 mm were cast using both the mix proportions. TMT bars of 10 mm dia in size and having a length of 100 mm were embedded at known cover. Before embedding, the initial weight of the rods was recorded. The covers of the concrete studied were 25, 40 and 50 mm. Both the top and bottom ends were sealed using the epoxy compound by leaving an exposed length of 85 mm. Electrical leads were taken and sealed. In one set of specimens, no chloride (0%) was added and in another set of specimens, 1% and 3% of sodium chloride by weight of cement was added at the time of casting. While casting, the rebars were embedded vertically with a 25 mm cover from the top and bottom. Duplicate specimens were cast for each strength and chloride concentration. The specimens were cured in potable water for 28 days at room temperature.

After 28 days of curing, the specimens were left under laboratory condition for 18 months till corrosion initiates and spreads uniformly on the rebar in chloride added concretes. At the end of the exposure, the rebar in 0%  $\text{Cl}^-$  added concrete was under passive condition whereas in 1% and 3%  $\text{Cl}^-$  added concrete was under active condition. Before electrochemical measurement, the specimens were conditioned by keeping them immersed in water for 48 h and dried at room temperature for 6 h to avoid too much dryness of the concrete.

### 2.3. Method of measurement

All the electrochemical measurements were carried out using three electrode assembly. Saturated calomel electrode (SCE) was used as a reference electrode and steel specimen/rebar embedded in the cement mortar/concrete acted as a working electrode. When making measurement in the cement extract, platinum electrode was used as a counter electrode (CE), whereas perforated stainless steel electrode (Dia × height: 75 mm × 60 mm) was used as CE when conducting the experiment on the cement mortar. Mortar

**Table 1**  
Details of concrete mix proportion.

Grade	Mix proportion	w/c ratio	Cement (kg m <sup>-3</sup> )	Water (kg m <sup>-3</sup> )	Fine aggregate (kg m <sup>-3</sup> )	Coarse aggregate (kg m <sup>-3</sup> )	28 days compressive strength (MPa)
M25	1:2.19:3.73	0.63	308	194	676	1148	31
M35	1:1.76:2.05	0.50	434	217	767	890	43

specimens were kept immersed in the cement extract solution and surrounded by CE during the measurement.

Stainless steel electrode (10 mm × 80 mm) was used as an auxiliary electrode when  $i_{\text{corr}}$  was measured on the rebars embedded in the concrete specimens. This was placed on a wetted sponge below which SCE was placed [27]. The length of the CE was more than the exposed length of the rebar and by means of this, the current was distributed uniformly throughout the length of the rebar [28,29]. Chloride solution was used as a contacting solution to reduce the contact resistance between the electrode assembly and the concrete.

2.3.1. Harmonic analysis (HA)

HA was carried out using ACM field machine – Version 5 (Advanced Corrosion Measurements, UK) that was operated by the ACM sequencer/core running/analysis V3 combined software. A sine wave with an ac amplitude of 20 mV ( $U_0$ ) and a frequency of 10 mHz were used when tested in mortar/concrete and 100 mHz in cement extract to perturb the system and the resultant first, second and third harmonic currents were determined. From the harmonic currents, the  $i_{\text{corr}}$  and Tafel slopes were calculated as below: [17,27].

$$i_{\text{corr}} = \frac{(i_1 + 3i_3)^2}{4\sqrt{3} |2(i_1 + 3i_3)i_3 - i_2^2|^{1/2}} \tag{1}$$

$$\frac{1}{b_{a,c}} = \frac{1}{4.6U_0} \left( \frac{i_1 + 3i_3}{i_{\text{corr}}} \pm 4 \frac{i_2}{i_1 + 3i_3} \right) \tag{2}$$

As suggested by Diard et al. [30] the third term in first harmonic current has been introduced which is three times the absolute value of the third harmonic current. As the mortar/concrete had a very high resistance, the IR compensation was carried out with an ac amplitude of 20 mV at the frequency of 10 kHz. In the sequencer list, the IR compensation set value was included along with the harmonic analysis. The polarization voltage would contain higher harmonic components, which would falsify the measuring results if IR compensation had not been carried out during the measurement [15]. Measurements were made on duplicate specimens and the average value was reported. As the cement extract has a negligible resistance, no IR compensation had been done. During the measurement PAIR (Phase and Impedance Reduction) option is “ON” by default thus the cable and instrumentation error was reduced by the PAIR calibration matrix.

2.3.2. Electrochemical impedance spectroscopy (EIS)

A small sinusoidal voltage signal of 20 mV was applied at the open-circuit potential over the frequency range of 30 kHz to 10 mHz using a computer controlled electrochemical analyzer (Model ACM Field machine, UK). The impedance values were plotted on the Nyquist plot. From the Nyquist plot, using the software ‘V-analysis’, the  $R_{\text{ct}}$  value was calculated from the diameter of the semi-circle extrapolated in the low frequency range between

100 Hz and 10 mHz [31,32]. By assuming  $B$  as 26 mV, the  $i_{\text{corr}}$  was calculated using the Stern–Geary relation [33],

$$i_{\text{corr}} = \frac{B}{R_{\text{ct}}} \tag{3}$$

where,  $B$  – Stern–Geary constant, 26 mV/decade for both active and passive state of rebar;  $R_{\text{ct}}$  – charge transfer resistance,  $\Omega \text{ cm}^2$ ;  $i_{\text{corr}}$  – corrosion current,  $\mu\text{A cm}^{-2}$ .

2.3.3. Tafel extrapolation technique (TET)

IR compensated potentiodynamic polarization was carried out by polarizing the rebar to  $\pm 200$  mV at the scan rate of 1 mV/s. The IR compensation was carried out with an ac amplitude of 20 mV at the frequency of 10 kHz. In the sequencer list, IR compensation set value was included along with the IR compensated custom sweep. The observed polarization curves were analyzed using the curve fitting programme and  $b_a$ ,  $b_c$ ,  $i_{\text{corr}}$  were determined. Then the values were compared with the values determined using HA.

All the above three measurements were carried out on the same specimen in the same sequential order as described above with 24 h interval between each technique.

2.3.4. Corrosion rate (CR) from weight loss method

After carrying out all the measurements, the concrete specimens were open and the rods were taken out. After pickling the rebars in inhibited hydrochloric acid as specified in ASTM G1 [34], the final weight was measured. From the initial and final weights, the corrosion rate in  $\mu\text{m y}^{-1}$  was calculated as:

$$\text{Corrosion rate in } \mu\text{m y}^{-1} = \frac{87,600 \times w}{dat} \tag{4}$$

where  $w$  – loss in weight, mg;  $d$  – density of iron,  $\text{g cm}^{-3}$ ;  $a$  – area,  $\text{cm}^2$ ;  $t$  – time, h.

The corrosion rate determined was compared that obtained through harmonic analysis.

3. Results

3.1. Harmonic analysis

3.1.1. Studies in cement extract and cement mortar

Table 2 compares the  $i_{\text{corr}}$  of steel in cement extract with the steel embedded in the cement mortar under both the passive (no chloride) and active condition (with chloride). At passive condition, the  $i_{\text{corr}}$  of steel in extract is  $0.240 \mu\text{A cm}^{-2}$  and increases to  $8.353 \mu\text{A cm}^{-2}$  in the presence of 1000 ppm of chloride. Similarly, in cement mortar, the  $i_{\text{corr}}$  of rebar is  $9.922 \mu\text{A cm}^{-2}$  in the presence of 3% of chloride, whereas it is  $0.1114 \mu\text{A cm}^{-2}$  in 0% chloride, respectively.

The frequency of the measuring voltage has been selected in order to satisfy two necessary conditions [17,35] viz., the imaginary component of the electrode impedance must be negligible in comparison to the real component i.e., less than 10% of the real component; the absolute value of the electrode impedance ( $|Z|$ ) should

**Table 2**  
Comparison of  $i_{\text{corr}}$  in cement extract and mortar: HA versus EIS and TET.

System	Frequency (mHz)	$U_0$ (mV)	HA						EIS			TET
			$i_1$ ( $\mu\text{A cm}^{-2}$ )	$i_2$ ( $\mu\text{A cm}^{-2}$ )	$i_3$ ( $\mu\text{A cm}^{-2}$ )	$i_{\text{corr}}$ ( $\mu\text{A cm}^{-2}$ )	$b_a$ (mV/decade)	$b_c$ (mV/decade)	$B$ (mV/decade)	$R_{\text{ct}}$ ( $\Omega \text{ cm}^2$ )	$i_{\text{corr}}$ ( $\mu\text{A cm}^{-2}$ )	$i_{\text{corr}}$ ( $\mu\text{A cm}^{-2}$ )
Cement extract	100	20	0.446	0.00282	0.00282	0.24	38	46	9	$1.132 \times 10^4$	0.7951	–
Cement extract + 1000 ppm $\text{Cl}^-$	100	20	0.1027	2.373	10.15	8.353	18	20	4	$1.29 \times 10^3$	3.1	–
Cement mortar + 0% Chloride	10	20	1.009	0.2896	0.00670	0.1114	36	143	13	$8.429 \times 10^4$	0.1542	0.1163
Cement mortar + 1% Chloride	10	20	2.469	0.0061	0.00097	0.6296	135	189	34	$2.214 \times 10^4$	1.5357	0.7923
Cement mortar + 3% Chloride	10	20	30.76	0.4174	0.00712	9.922	178	226	43	$3.748 \times 10^3$	11.4728	9.94

not differ significantly from the polarization resistance. At the selected frequency, the reactive component of the current is small as compared to the Faradaic component. In the present study, the choice of the frequency is made on the basis of the impedance diagram. Figs. 1 and 2 compare the Nyquist plot of steel in cement extract and mortar whereas Figs. 3 and 4 compare the Bode plot of the same. In the absence of chloride, the Nyquist plot shows the capacitive nature of the passive film ( $\gamma\text{-Fe}_2\text{O}_3$ ) formed on the rebar surface (Fig. 2) with a large time constant indicative of passive steel. The observed impedance is the result of the slow diffusion of oxygen through the mortar matrix, the dielectric film component results of the solid calcium hydroxide layer at the steel-mortar interface and the mortar. In the cement mortar containing 1% of chloride, the Nyquist plot yields a semi-circle indicating the breakdown of dielectric film due to chlorides. As shown in Fig. 2, the addition of chloride decreases the charge transfer resistance. Perhaps it indicates the competition between the aggressive chloride ions and the passivating hydroxyl ions. In the presence of 3% of chloride, depressed semi-circle is observed.

Data extracted from the Figs. 1–4 is given in Table 3 to verify whether the condition necessary for HA measurement is satisfied or not. Comparison has been made both at 100 mHz and 10 mHz. From the data it is clearly evident that when the rebar is in passive condition, the value of  $Z''$  is more than 10% of  $Z'$  at both frequencies and hence the conditions are not satisfied. But when the rebar attains active condition and comes under the charge transfer controlled reaction, at the frequency of 100 mHz in the cement extract and at 10 mHz in the cement mortar, the conditions are satisfied. For example, in cement extract in the presence of 1000 ppm of chloride, value of  $Z''$  is 0 at 100 mHz i.e., almost negligible compared to  $Z'$  and the value of total impedance  $|Z|$  is  $1290 \Omega \text{ cm}^2$  which is almost equal to the value of  $R_{ct}$  (Fig. 3). But in the cement mortar, containing 3% of chloride, the value of  $Z''$  is 23% of  $Z'$  at 10 mHz and the value of  $|Z|$  is not exactly equal to  $R_{ct}$ . The resistance of mortar is considerably higher than that of extract and thus introduces another time constant in the Nyquist plot. This is clearly seen by comparing the Fig. 1 with Fig. 2. The value of  $Z'' < Z'$  only when the frequency is 10 mHz at both 1% and 3% chloride concen-

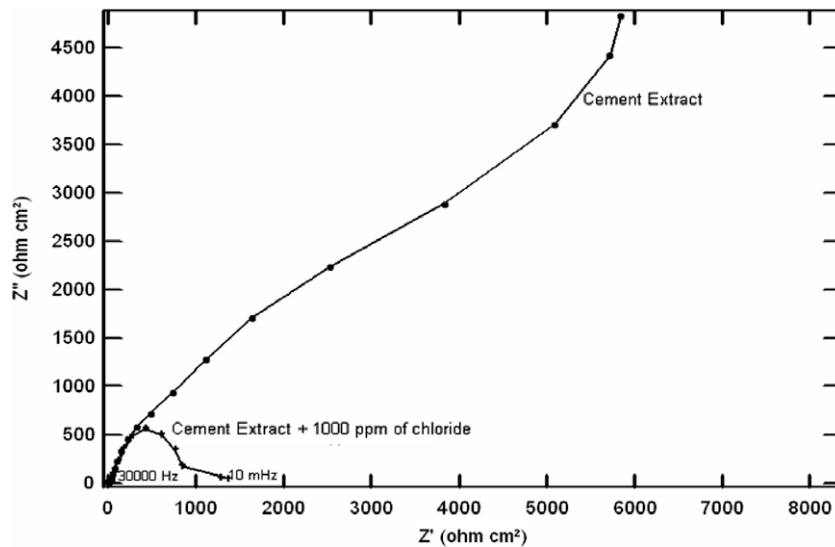


Fig. 1. Nyquist plot of steel specimen in cement extract.

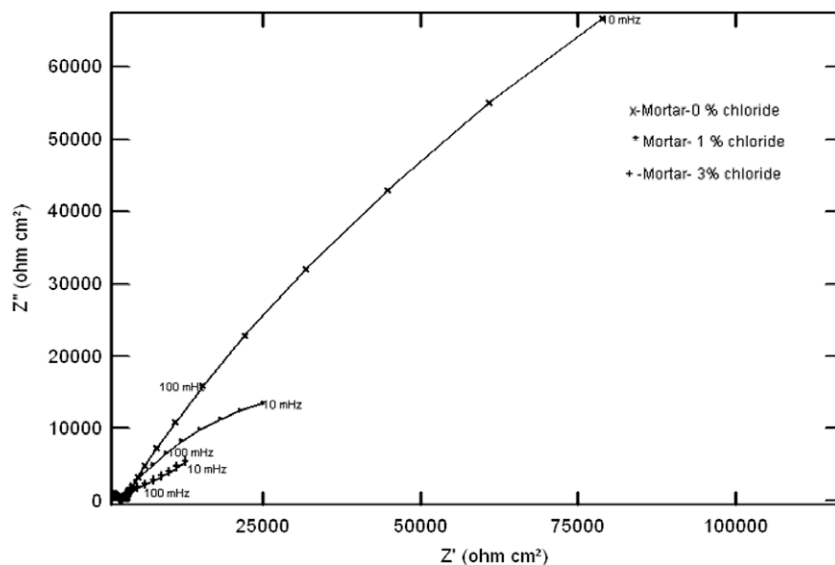


Fig. 2. Nyquist plot of rebar embedded in cement mortar.

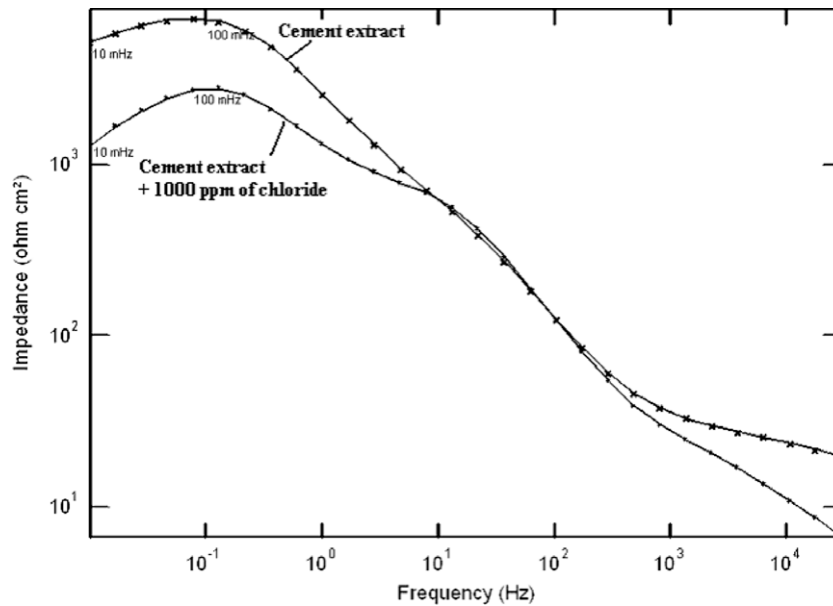


Fig. 3. Bode plot of steel in cement extract.

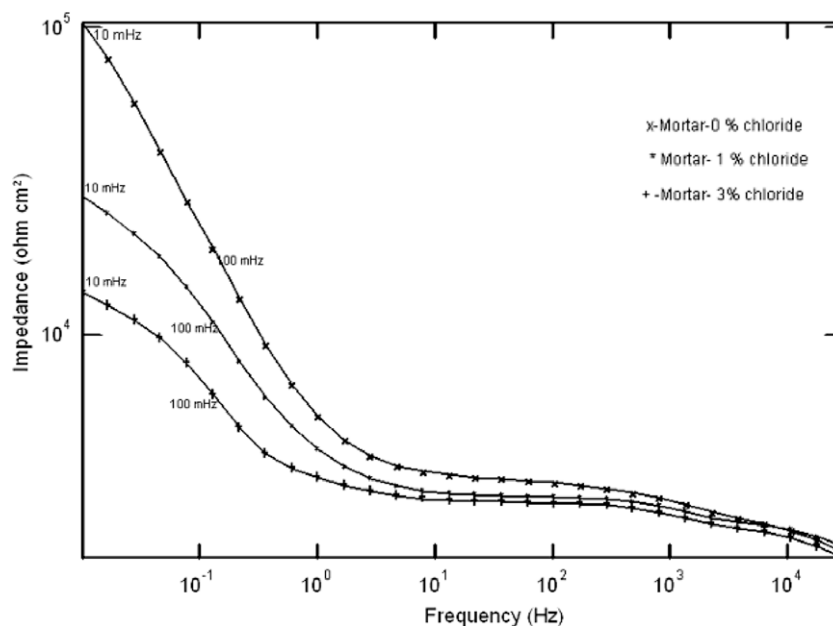


Fig. 4. Bode plot of rebar embedded in cement mortar.

trations. Due to this reason, a frequency of 10 mHz was selected to conduct the experiment in the cement mortar. When compared to 100 mHz at 10 mHz, the current due to Faradaic current is higher than the current due to reactive components. Due to this, the error is minimum at 10 mHz when compared to 100 mHz. Even at higher  $i_{\text{corr}}$  of  $9.9 \mu\text{A cm}^{-2}$ , the value of  $|Z|$  modulus is not exactly equal to  $R_{\text{ct}}$  (Fig. 4). This condition is satisfied in highly corrosive medium ( $i_{\text{corr}} > 100 \mu\text{A cm}^{-2}$ ), when the reaction is purely activation controlled [35]. But in the case of rebar embedded in mortar (iron in alkaline medium) where the rate of dissolution is less, the  $|Z|$  is not exactly equal to  $R_{\text{ct}}$ . However when the experiment is conducted at the frequency of around 1 mHz, the value of  $|Z|$  is exactly equal to  $R_{\text{ct}}$  and the value of  $Z''$  is almost zero. But at this low frequency it is difficult to measure  $i_{\text{corr}}$  because it is time consuming (more than 60 min) and also possible misinterpretation due to electrochemical noise.

Fig. 5 compares the Tafel plot of steel embedded in the cement mortar containing 0%, 1% and 3% of chloride. From the figure it is observed that  $E_{\text{corr}}$  is shifted to more negative direction due to the addition of chloride. The value is  $-200 \text{ mV}$ ,  $-320 \text{ mV}$  and  $-550 \text{ mV}$  in 0%, 1% and 3% of chloride, respectively. As seen from Table 2, the  $i_{\text{corr}}$  of steel in the cement mortar predicted by the HA was compared with the EIS and TET, the  $i_{\text{corr}}$  by HA and TET are nearly equal whereas it is higher by EIS. This is observed under both passive and active conditions of the rebar.

### 3.1.2. Studies on concrete

3.1.2.1. Selection of frequency. Table 4 compares the  $Z''$  with  $Z'$  at different frequencies in M25 concrete at 25 mm cover. In M25–0%  $\text{Cl}^-$  added concrete due to the presence of Warburg impedance, the conditions are not satisfied at both the frequencies i.e.,  $Z''$  is  $>10\%$  of  $Z'$ . In the case of 3%  $\text{Cl}^-$  added concrete, the condition is

**Table 3**  
Comparison of  $Z'$  and  $|Z|$  in the cement extract and mortar.

System	Condition of steel	Frequency (mHz)	$Z'$ ( $\Omega \text{ cm}^2$ )	$Z''$ ( $\Omega \text{ cm}^2$ )	Value of $Z''$ w.r.t. $Z'$ (%)	$ Z $ ( $\Omega \text{ cm}^2$ )	$R_{ct}$ ( $\Omega \text{ cm}^2$ )
Cement extract	Passive	100	6203	4504	72.61	7665	11,340
		10	5175	3154	60.95	–	–
Cement extract + 1000 ppm of chloride	Active	100	3175	0	0	1290	1284
		10	1289	52	4.02	–	–
Cement mortar + 0% chloride	Passive	100	11,727	13,303	$Z'' > Z'$	–	–
		10	78,973	66,720	84	76,614	84,290
Cement mortar + 1% chloride	Active	100	8513	6125	72	–	–
		10	25,102	13,432	54	28,470	22,140
Cement mortar + 3% chloride	Active	100	5810	1248	21	–	–
		10	11,889	2684	23	12,188	3748

satisfied at both 100 mHz and 10 mHz frequencies. But, for the comparison of  $i_{\text{corr}}$  of rebar at passive with the active condition, 10 mHz has been selected since  $i_{\text{corr}}$  is dependent on frequency. In M25 concrete, at the frequency of 5 Hz, though the value of  $Z''$  is insignificant i.e., 2–4% that of  $Z'$ , the current from the reactive components is almost negligible only at low frequency. Due to this, the  $i_{\text{corr}}$  at 10 mHz is nearing very close to the value determined by EIS and TET than that at 5 Hz (Table 5). In M35 concrete at 5 Hz, the  $i_{\text{corr}}$  of passive and active rebar is  $1.109 \mu\text{A cm}^{-2}$  and  $1.193 \mu\text{A cm}^{-2}$ , respectively, and there is no significant change between them. As seen from the Bode plot (Fig. 6), the  $|Z|$  is not equal to  $R_{ct}$  both at passive and active conditions.

At higher frequency, double layer capacitance ( $C_{dl}$ ) at the interface acts as a least resistance path and most of the current passes through it rather than through the charge transfer resistance  $R_{ct}$ . At lower frequency only, the measured  $i_{\text{corr}}$  is free from the charging current. In addition to this, the frequency above 1 Hz reflected mainly the conductance properties of the concrete and was hardly influenced by the charge transfer resistance of the rebar. Hence, the changes that occur at the steel–concrete interface can be easily identified only at the low frequency. Due to these reasons, it appears that the frequency of 10 mHz is more appropriate than 100 mHz for the accurate determination of  $i_{\text{corr}}$  though it is not satisfied the conditions.

**3.1.2.2. Selection of amplitude.** Selection of the amplitude  $U_0$ , must be in such a way that it should reach steady state condition and be capable of accurately measuring the second and third harmonic

components. Table 5 compares the  $i_{\text{corr}}$  of rebar in M25 and M35 concrete at the chloride levels of 0% and 3% at 25 mm cover. The data implies that  $i_{\text{corr}}$  is dependent on amplitude. If the amplitude is increased from 20 to 30 mV, the  $i_{\text{corr}}$  of passive rebar is increased from  $0.234$  to  $0.470 \mu\text{A cm}^{-2}$ . When comparing the  $i_{\text{corr}}$  at 30 mV, it is  $0.470$  and  $0.3744 \mu\text{A cm}^{-2}$  in passive and active condition of rebar, respectively, and the change in value is insignificant when the condition of rebar is changed from passive to active. But at 20 mV, the  $i_{\text{corr}}$  of active rebar is 6.5 times higher than that of the passive rebar, thus able to be differentiated clearly the active condition from passive condition. Hence it infers that amplitude of 20 mV is more appropriate than 30 mV. In addition to this, it has been also suggested that the values shall be between  $\beta/2$  and  $\beta$  (where  $\beta$  equals  $b_a/2.303$  or  $b_c/2.303$  whichever is smaller) are suitable [15]. Accordingly in the present study, the value varies between 11 and 37 mV ( $\beta/2 - \beta$ ) depends upon the cover of the concrete and the state of the rebar. The selected amplitude of 20 mV lies between 11 and 37 mV.

From the foregoing discussion it can be understood that  $i_{\text{corr}}$  measurement at a frequency of 10 mHz with an amplitude of 20 mV is more reliable using HA under both active and passive conditions of the rebar.

### 3.2. Electrochemical impedance spectroscopy (EIS)

Figs. 7 and 8 compare the Nyquist plot of rebar embedded in M25 and M35 concretes at 25 mm cover, respectively. As seen from the plots, there are two time constants; one is from high frequency

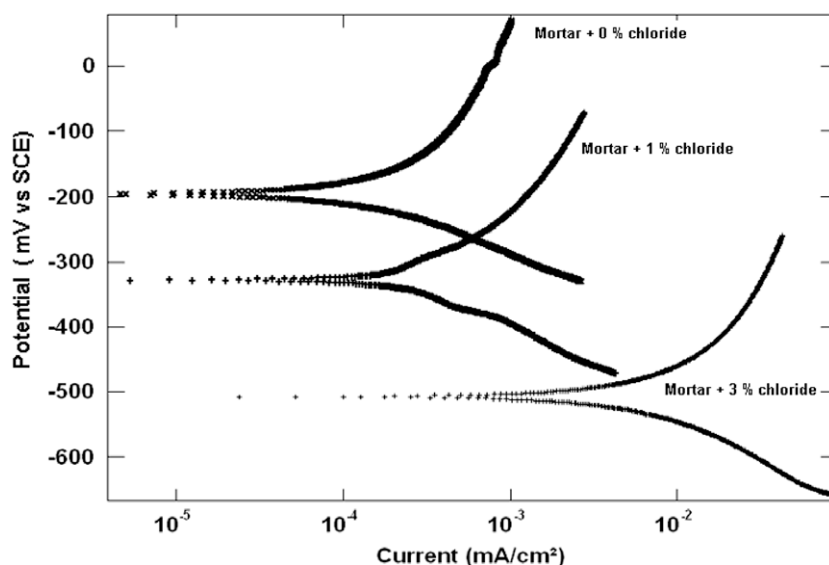


**Fig. 5.** Tafel plot of rebar embedded in cement mortar specimens.

**Table 4**  
Comparison of  $Z'$  and  $|Z|$  in M25 concrete (25 mm cover).

System	Condition of steel	Frequency (Hz)	$Z'$ ( $\Omega \text{ cm}^2$ )	$Z''$ ( $\Omega \text{ cm}^2$ )	Value of $Z''$ w.r.t. $Z'$ (%)	$ Z $ ( $\Omega \text{ cm}^2$ )	$R_{ct}$ ( $\Omega \text{ cm}^2$ )
M25 concrete + 0% chloride	Passive	0.1	36,445	6278	17	–	–
		0.01	51,117	50,993	99	72,161	152,300
		5	32,731	1336	4.08	–	–
M25 concrete + 3% chloride	Active	0.1	21,128	980	4.6	–	–
		0.01	22,869	2463	11	22,869	16,600
		5	19,885	349	1.76	–	–

**Table 5**  
Comparison of  $i_{\text{corr}}$  versus  $U_0$  (at 25 mm cover).

System	Condition of the rebar	Frequency (Hz)	Amplitude $U_0$ , (mV)	$i_1$ ( $\mu\text{A cm}^2$ )	$i_2$ ( $\mu\text{A cm}^2$ )	$i_3$ ( $\mu\text{A cm}^2$ )	$i_{\text{corr}}$ ( $\mu\text{A cm}^2$ )		
							HA	EIS	TET
M25 concrete + 0% chloride	Passive	0.01	20	8.263	0.5721	0.2051	0.234	0.0853	0.0206
		0.01	30	10.81	2.123	0.00524	0.470	–	–
M25 concrete + 3% chloride	Active	0.01	20	45.29	0.4771	0.9476	1.514	1.205	1.385
		0.01	30	14.53	2.284	0.6188	0.374	–	–
M25 concrete + 0% chloride	Passive	5	20	13.99	0.1694	0.3015	0.401	0.0853	0.0206
M25 concrete + 3% chloride	Active	5	20	34.56	0.2490	0.2383	1.645	1.205	1.385
M35 concrete + 0% chloride	Passive	0.01	20	10.29	0.4394	0.1061	0.424	0.4672	0.0142
M35 concrete + 3% chloride	Active	0.01	20	32.5	1.989	0.3669	1.342	1.855	1.343
M35 concrete + 0% chloride	Passive	5	20	33.61	0.2302	0.5182	1.109	0.4672	0.0142
M35 concrete + 3% chloride	Active	5	20	43.31	1.053	1.043	1.193	1.855	1.343

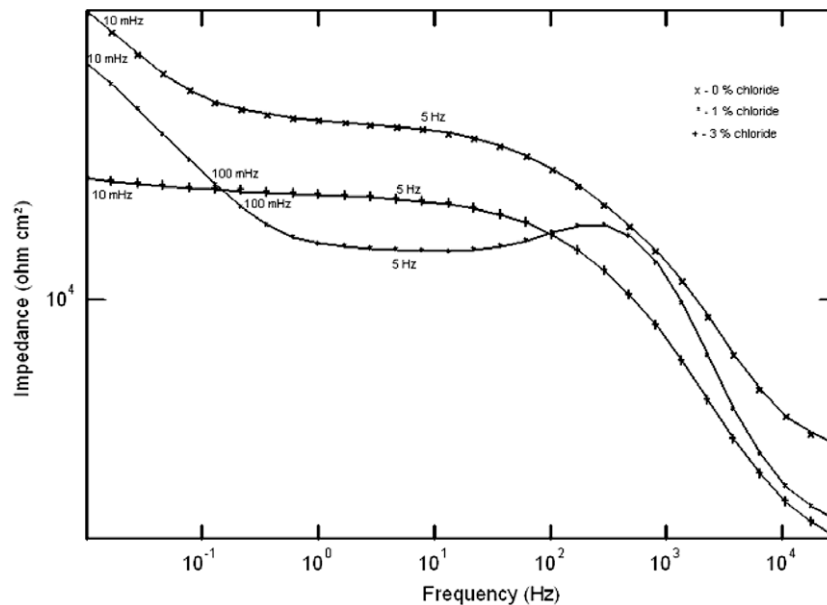


**Fig. 6.** Bode plot of rebar embedded in M25 concrete at 25 mm cover.

region (30 kHz to 100 Hz) contributed by the resistance of the concrete and another one is from low frequency region (100 Hz to 10 mHz) due to charge transfer resistance from the rebar. It can be also seen from the figures, the slope of the low frequency arc decreases as the chloride concentration is increased. In 0%  $\text{Cl}^-$  added concrete, the rebar response shows mainly capacitive behaviour with large charge transfer resistance and large diffusion impedance indicative of passive steel. In the presence of 1% and 3% of chloride, when corrosion occurs on the rebar, the rebar comes under charge transfer controlled reaction with low charge transfer resistance and low diffusion impedance. After extrapolating of the semi-circle plot to the real axis, the  $R_{ct}$  value was determined. Using the  $B$  value calculated from HA, the  $i_{\text{corr}}$  was determined and compared

with the  $i_{\text{corr}}$  from HA and given in Fig. 9. The correlation co-efficient ( $R^2$ ) and slope nearing close to 1, which indicates that  $i_{\text{corr}}$  from HA is nearly equal to  $i_{\text{corr}}$  by EIS.

By assuming  $B$  as 26 mV, the  $i_{\text{corr}}$  was determined and compared with the  $i_{\text{corr}}$  by HA and given in Fig. 10. The ' $R^2$ ' value is 0.7428 deviated much from 1 indicates an insignificant correlation, especially for the higher  $i_{\text{corr}}$  value. It shows that assumed  $B$  value leads to an error in calculating  $i_{\text{corr}}$ . Because  $B$  value not only depends upon the condition of the rebar but also on the reduction reaction at cathode, which in turn depends upon the oxygen availability near the cathode. Data also reiterate that  $B$  value cannot be assumed as it varied depending upon the  $i_{\text{corr}}$  values.

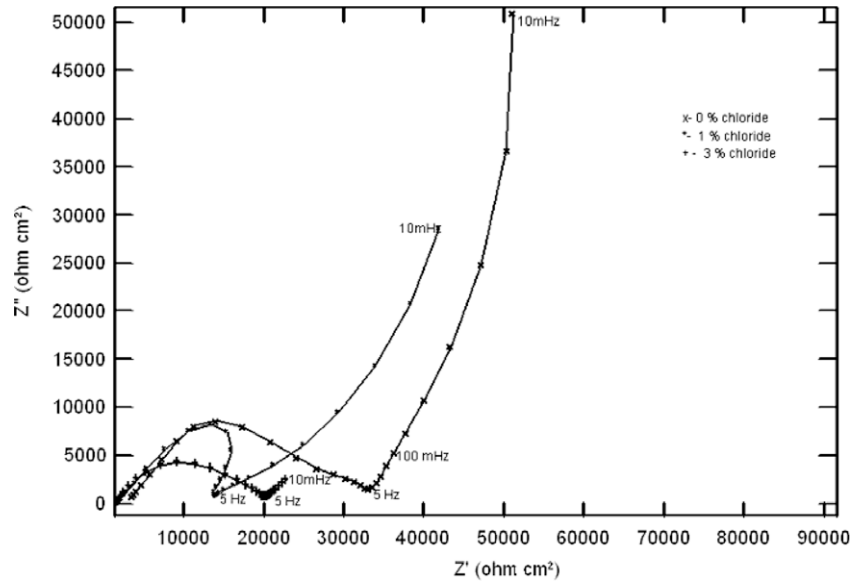


Fig. 7. Nyquist plot of rebar embedded in M25 concrete at 25 mm cover.

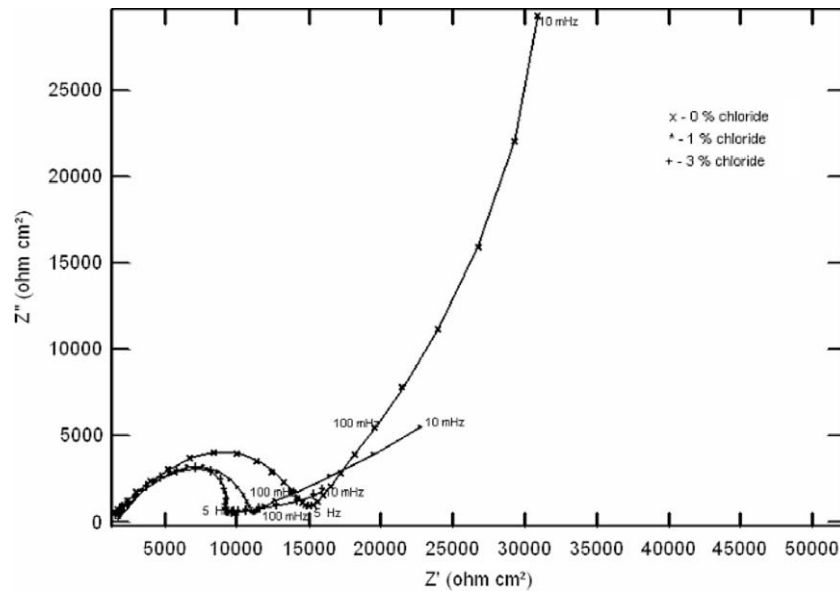


Fig. 8. Nyquist plot of rebar embedded in M35 concrete.

### 3.3. Tafel extrapolation technique (TET)

Figs. 11–14 show the polarization behaviour of rebar in M25 and M35 concrete in 0% and 3% chloride, respectively. In 0%  $\text{Cl}^-$  added concrete (Figs. 11 and 13), the passive region is higher whereas in the presence of 3% chloride (Figs. 12 and 14), there is no passive region. The  $i_{\text{corr}}$  of TET with the  $i_{\text{corr}}$  of HA has been compared in Fig. 15. As seen from Table 5, at passive condition, the  $i_{\text{corr}}$  by TET is 10 times less than that of by HA. This may be probably due to the passivation of rebar in concrete at the higher anodic potential. For example in HA the rebar was polarized +20 mV from the open-circuit potential whereas in TET it was  $\pm 200$  mV on both the anodic and cathodic side. Whereas at active condition, TET and HA showed the similar results.

### 3.4. B value

#### 3.4.1. From HA

Fig. 16 compares the variation of  $B$  value with the  $i_{\text{corr}}$ . It is evident from the figure that  $B$  value does not decrease linearly to 26 mV from the value of 52 mV when the rebar attains the active state from passive. The average  $B$  value of rebar from HA measurement at passive condition is  $19 \pm 5$  mV whereas it is  $23 \pm 9$  mV at active condition. In contrary to the reported value of 52 mV for passive steel, a value of 19 mV was obtained in M35 concrete and 24 mV was obtained in M25 concrete. In the absence of chloride, the  $B$  value is 13 in cement mortar and the value is still reduced to 9 in cement extract (Table 2). The continuous formation of self-generating protective layer  $\gamma\text{-Fe}_2\text{O}_3$  at the steel–concrete

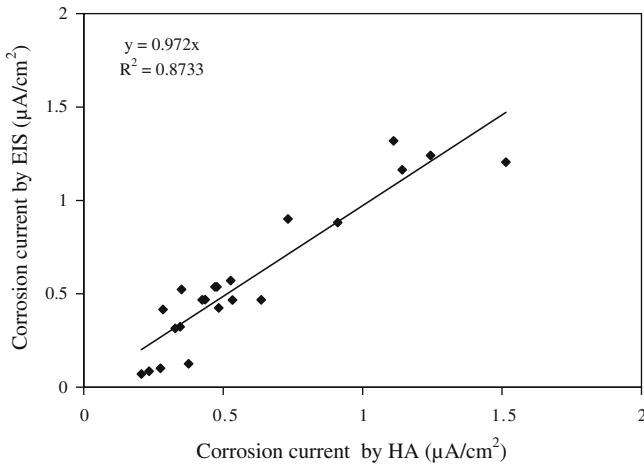


Fig. 9. Comparison of corrosion current: HA versus EIST (substituting HA determined B value).

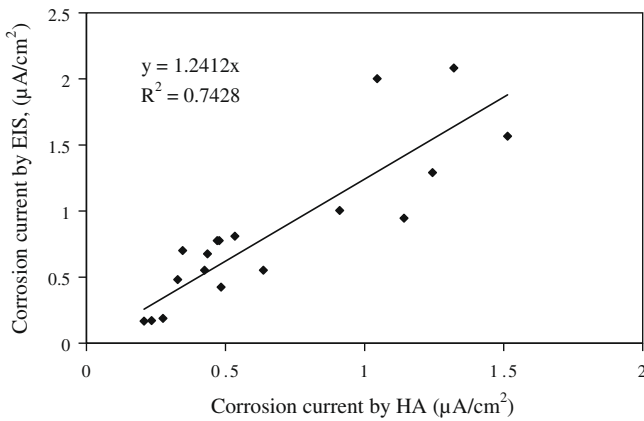


Fig. 10. Comparison of corrosion rate: HA versus EIST (assumed B value as 26 mV).

interface is possible in the cement extract and mortar and it is not possible in the concrete due to the presence of coarse aggregate.

Discontinuity on the passive layer and slow diffusion of O<sub>2</sub> through the concrete matrix are the probable reasons for higher values of B in concrete than that of mortar.

In the presence of chloride, when corrosion occurs, Fe<sup>2+</sup> ions are released, which react with the water molecules in the pore solution giving Fe(OH)<sub>2</sub> as shown below:



The release of H<sup>+</sup> ions acidifies the pore solution surrounding the rebar. As reported by Garces [7], if the *i*<sub>corr</sub> was between 5 and 40 µA cm<sup>-2</sup>, then the pH of the pore solution was in the range of 5–9.5. The formation of Fe(OH)<sub>2</sub> tends to fix a pH of 9.5 on the steel surface. They also observed a higher B value of 37 mV in synthetic pore solution in the presence of 0.02 M chloride. In the present study, the rebar in mortar containing 3% chloride shows the *i*<sub>corr</sub> and B is 9.922 µA cm<sup>-2</sup> and 43 mV, respectively. Hence the B value also depends upon the pH of the pore solution. In concrete, as shown in Table 6, as there is no trend, it seems the presence of chloride and cover of concrete does not have any influence on the B value. Similar behaviour is observed in M25 concrete also. The Tafel slopes are distorted by the contributions of slow diffusion processes of oxygen as well as by galvanic interactions [36].

3.4.2. From TET

For a ‘corroding system’ where the anodic and cathodic partial reactions are purely charge transfer controlled, the Stern–Geary constant is defined as:

$$B = \frac{b_a \times b_c}{2.303(b_a + b_c)} \quad (6)$$

where *b*<sub>a</sub> – anodic Tafel constant, mV/decade; *b*<sub>c</sub> – cathodic Tafel constant, mV/decade; B – Stern–Geary constant, mV/decade.

The anodic and cathodic Tafel constants *b*<sub>a</sub> and *b*<sub>c</sub> in this case would be

$$b_a = \frac{2.303RT}{ZF}; \quad b_c = \frac{2.303RT}{\alpha ZF} \quad (7)$$

using α (symmetry factor) = 0.5 and Z = 1 for both anodic and cathodic part of the electrochemical reactions, we get, theoretically

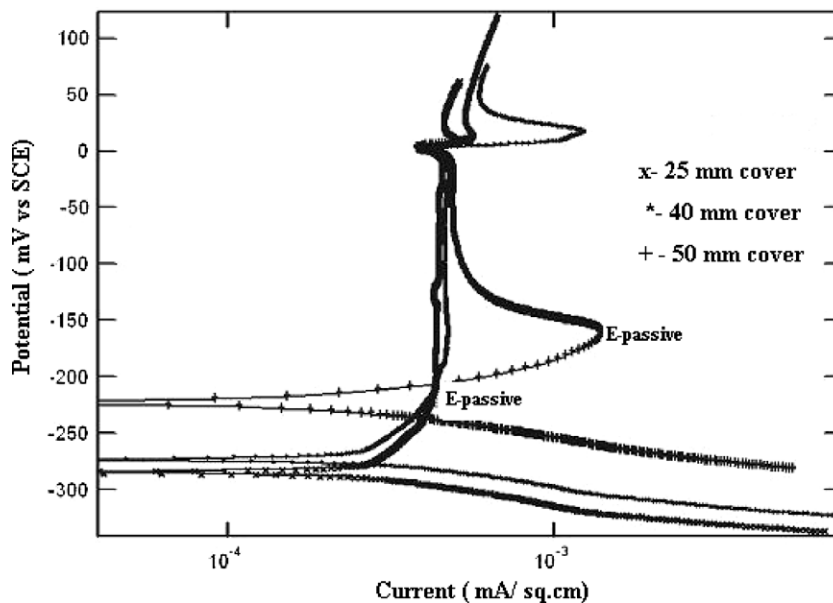


Fig. 11. Tafel plot of rebar in M25 concrete-0% chloride.

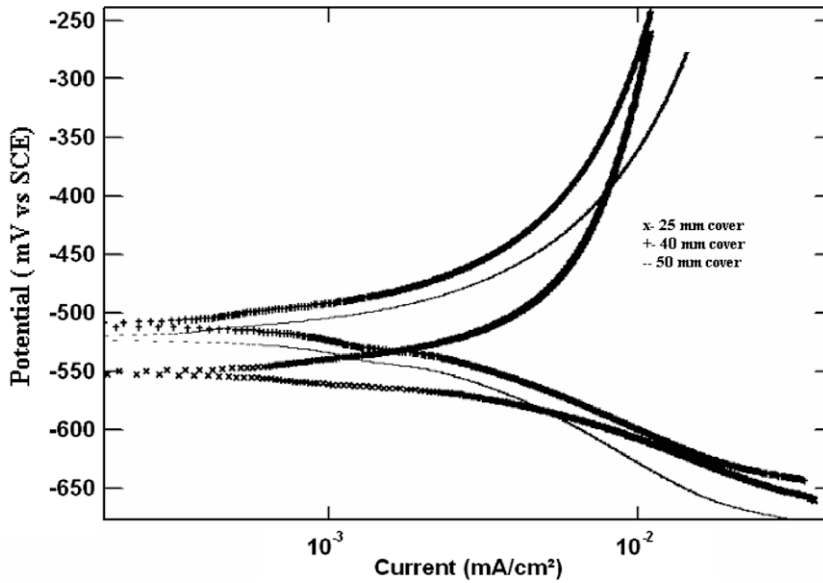


Fig. 12. Tafel Plot of rebar embedded in M25 concrete-3% chloride.

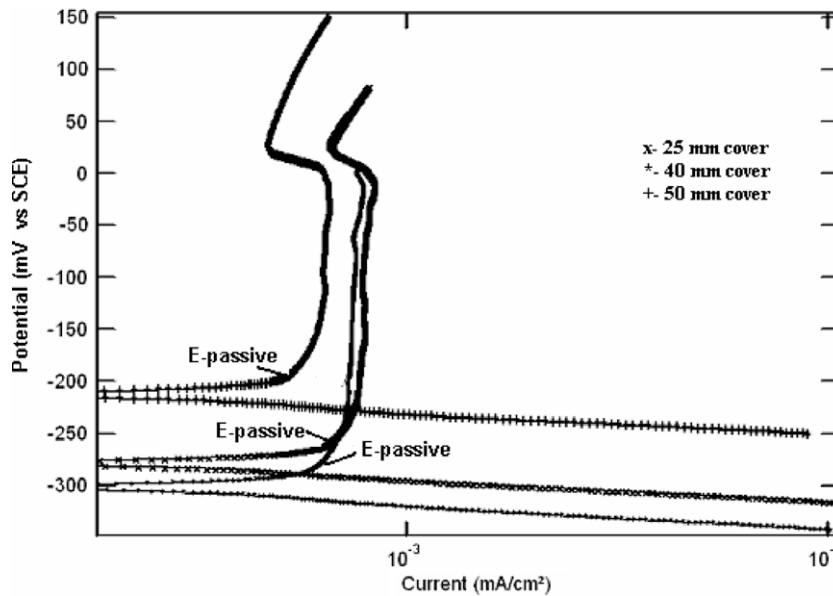


Fig. 13. Tafel plot of rebar in M35 concrete-0% chloride.

$$B_{\text{active}} = \frac{RT}{F} = 26 \text{ mV/decade}; \quad B_{\text{passive}} = \frac{RT}{\alpha F} = 52 \text{ mV/decade} \quad (8)$$

However for the system ‘corroding of steel in concrete’ the current-potential relation in some potential regions is more complicated (Figs. 11 and 12). The Tafel constants for the linear cathodic regions are typically very high due to the diffusion controlled oxygen reduction. For such diffusion controlled reactions, the Butler-Volmer equation is only valid at low over potentials which makes it impossible to evaluate the corrosion current density as well as Tafel slopes by extrapolation. In such a situation as suggested by Pruckner [37], the  $B$  was determined from the results of the other measurement techniques as below:

$$B = i_{\text{corr,Tafel}} \times R_{\text{ct,EIST}} \quad (9)$$

$E_{\text{corr}}$ ,  $b_a$  and  $b_c$  are determined from the entire curve by ‘non-linear least square curve fitting using Lev-Mar fit VI (Levenberg-Marqu-

ardt fit) [38]. In Fig. 17, the experimental data of polarization behaviour of rebar embedded in M25-3% Cl<sup>-</sup> added concrete is fitted with the Butler-Volmer equation. Then  $i_{\text{corr}}$  was determined by extrapolating  $b_a$  and  $b_c$  to the  $E_{\text{corr}}$  in the Tafel plot. Then using Eq. (9), the  $B$  was determined. Table 6 compares the  $B$  determined from HA with the value from using Eq. (8) in M35 concrete. From the data, it can be inferred that in most of the cases  $B$  from HA is very close to the value from Eq. (8) in 0% and 1% chloride added concrete whereas more deviation is observed in 3% chloride.

#### 4. Discussion

##### 4.1. First harmonic current

As reported in earlier investigations [15,16], the next term of first harmonic current has not been included in the determination of  $i_{\text{corr}}$  and Tafel constants. But in the present investigation  $i_1$  com-

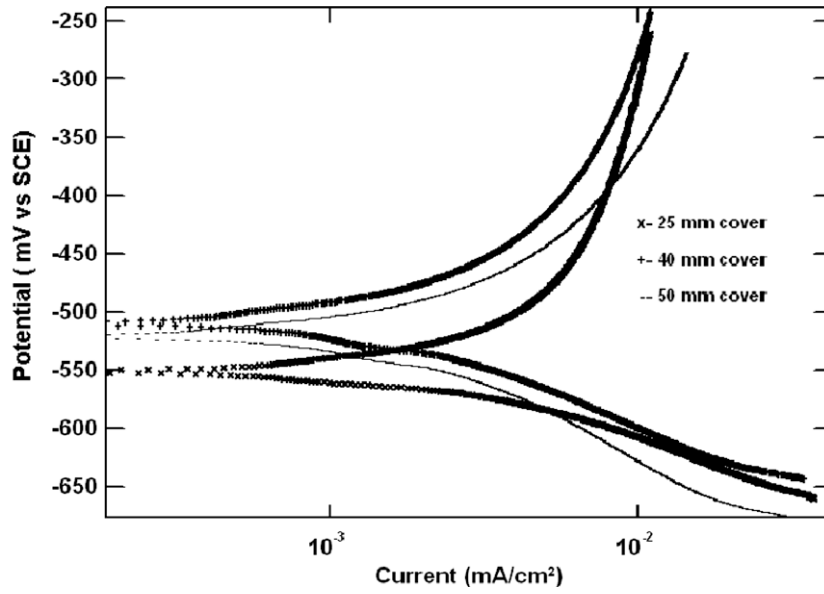


Fig. 14. Tafel plot of rebar in M35 concrete-3% chloride.

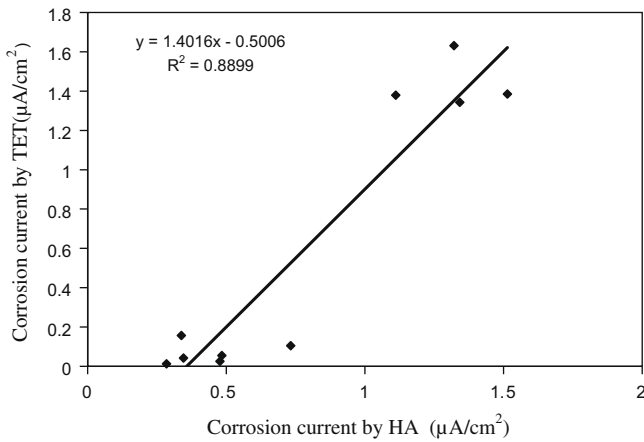


Fig. 15. Comparison of corrosion current: HA versus TET.

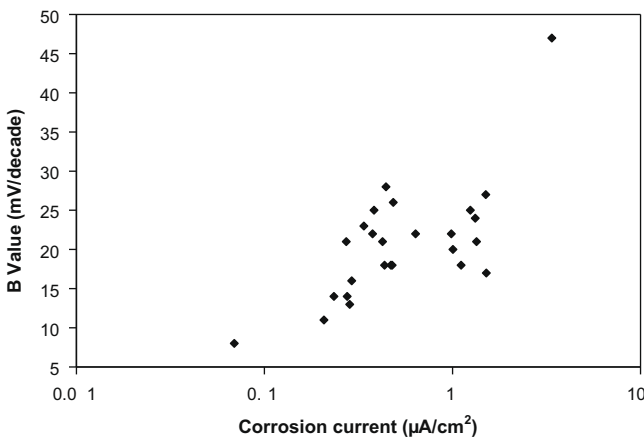


Fig. 16. Variation of B value with corrosion current.

Table 6 Comparison of 'B' value in M35 concrete: HA versus from Eq. (8).

Technique	0% chloride			1% chloride			3% chloride		
	Cover (mm)			Cover (mm)			Cover (mm)		
	25	40	50	25	40	50	25	40	50
Harmonic analysis	22	16	18	13	12	17	24	51	25
From Eq. (8)	22	15	31	11	13	18	17	18	16

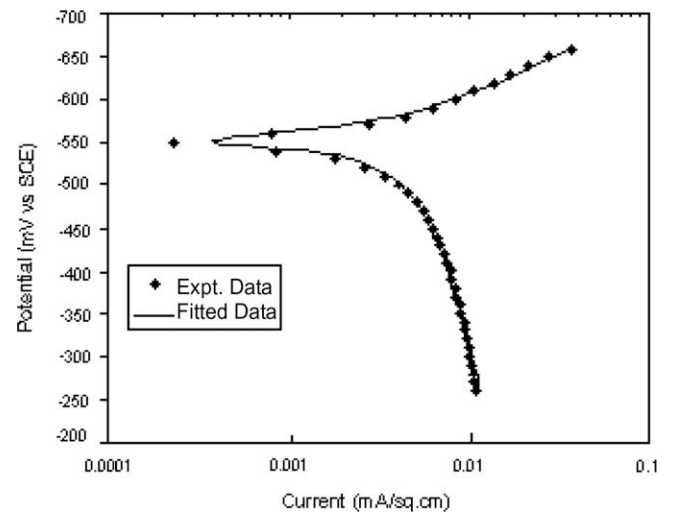


Fig. 17. Tafel plot of rebar in M25-3% Cl<sup>-</sup> added concrete: experimental data versus fitted data.

(i)  $\frac{3i_3}{i_1} > 0.01$ . (10)

ponent has been modified as given in Eqs. (1) and (2) due to the following reasons:

(ii) The rebar is under mixed diffusion and charge transfer control at low chloride concentration near the rebar. Under such complicated kinetic condition it is necessary to modify the  $i_1$  component for more accurate prediction of  $i_{corr}$ .

**Table 7**  
Comparison of corrosion rate: HA versus weight loss method.

System	Corrosion rate ( $\mu\text{m y}^{-1}$ )					
	Harmonic analysis			Weight loss method		
	Cover (mm)					
	25	40	50	25	40	50
M25–0% chloride	2.6	4.3	4.2	0	0	0
M25–3% chloride	11.6	6.1	13.2	11	7.2	11.2
M35–0% chloride	6.2	7	5.5	0	0	0
M35–3% chloride	17.4	25.3	14.4	16.5	8.1	11.3

#### 4.2. Effect of double layer capacitance

When measuring the harmonic currents, the electrode current also contains the harmonic components caused by the non-linear reactive part of the electrode impedance namely double layer capacitance ( $C_{dl}$ ) and pseudo capacitance even in the case of the right choice of the measuring frequency. In concrete, pseudo capacitance arises due to the adsorption of  $\text{OH}^-$ ,  $\text{K}^+$ ,  $\text{Na}^+$  and  $\text{Ca}^+$  ions on the rebar surface. If there is no double layer capacitance then there will be no frequency dependence. But data presented in Tables 2 and 5 confirm that  $i_{\text{corr}}$  is dependent on frequency. Since the adsorption process may have large time constants, the reactive part of the harmonic components cannot be eliminated completely. But fortunately these components are out of phase with respect to those of the Faradaic current i.e., first three reactive harmonic components correspond to terms  $\cos \omega t$ ,  $\sin 2\omega t$  and  $\cos 3\omega t$  of the Fourier series of the electrode current. Hence, the current measured is free from non-Faradaic current, since it is  $90^\circ$  out of phase with the applied voltage. For reliable measurement of  $i_{\text{corr}}$ , the charge transfer resistance  $R_{ct}$  should be less than  $(C_{dl}\omega)^{-1}$  [39]. At the frequency of 10 MHz, the condition is fulfilled both passive and active conditions of rebar thus ensuring the measured current passes through the charge transfer resistance rather than  $C_{dl}$ .

#### 4.3. Reliability of HA technique

Table 7 compares the CR determined by weight loss method with the HA. Both the values are nearing very close to each other. Since chloride has been added initially, the corrosion rate is almost equal at all covers because of uniform chloride concentration near the rebar. But the effect of cover has been taken as one of the parameters with the aim to know whether the selected frequency and amplitude in HA measurement is able to predict the  $i_{\text{corr}}$  accurately at higher covers. The data given in Table 7 suggest that the results of HA method are reliable up to 50 mm cover of concrete at the frequency of 10 MHz with an amplitude of 20 mV. At passive condition of rebar determination of CR is not accurate using weight loss method because of the presence of passive film and hence it appears that the CR given by HA is reasonable. But at active condition of rebar when embedded in concrete containing 3% of chloride, the CR by HA is higher by 5% at 25 mm cover whereas it is 15% and 27% higher at the cover of 40 and 50 mm, respectively, than that of weight loss method.

In actual field structures, if the chloride is already diffused inside the concrete, conducting TET at site may cause corrosion of the rebar when anodically polarizing the rebar to 200 mV. In uncontaminated concrete (passive rebar), the determination of anodic Tafel slope also may have some error because of the possible passivation of the steel at higher anodic polarization. The most important sources of error are the following: (a) erroneous estimation of the Tafel slopes or their determination by extrapolation due to selection of region and (b) current–potential characteristics dif-

fering from the Butler–Volmer relationship. These limit the use of TET at site for determining  $i_{\text{corr}}$  of rebar in concrete structures.

Similarly in EIS technique interpretation of data is more difficult if more than one time constant is involved. Dispersion of time constant caused the depressed semi-circle in the Nyquist plot. Concentration effects associated with the Warburg impedance mask the charge transfer resistance. It requires the collection of data at low frequencies, which leads to long measurement times and significant electrode disturbance both of which are unsuitable for practical on-site monitoring.

In HA technique, the time of measurement is only half-an hour with ACM field machine. In addition to direct measurement of  $i_{\text{corr}}$ , HA also has the advantage of permitting the determination of Tafel slopes at the corrosion potential using a very small perturbation of 20 mV. The Tafel slopes determined by extrapolation from the polarization curve are generally unreliable as the polarization of the rebar by several hundreds of millivolts from the equilibrium potential may substantially alter the character of the electrode processes. But practically, in the rebar corrosion rate assessment, prediction of corrosion rate is more important than Tafel slopes. The assumed  $B$  value as 26 mV arrived based on unreliable experiments or calculation introducing 2–4 times error when converting  $R_{ct}$  into a  $i_{\text{corr}}$  (Fig. 11). In the present investigation it has been proved that corrosion rate data obtained by the HA technique are in good agreement with those calculated by EIS and weight loss method and thus free from errors. In actual concrete structures, where the length of the rebar is more than that of CE, guard ring probe [6,29] shall be used to confine the electrical signal to the known rebar length.

## 5. Conclusions

Based on the detailed investigations carried out on M25 and M35 grades concrete, cement mortar and extract, the following broad conclusions are drawn:

1. Studies conducted on the rebar embedded in the cement mortar and concrete at the chloride concentration of 0%, 1% and 3% show that corrosion rate data determined by HA at 10 MHz with an ac amplitude of 20 mV is comparable to that of by EIS and weight loss method. Whereas corrosion rate predicted by TET is 10 times lower under passive state of the rebar (0%  $\text{Cl}^-$  added concrete) but very close to the value by HA under active state of the rebar (3%  $\text{Cl}^-$  added concrete).
2. The conditions necessary for HA measurements are satisfied, only when the rebar is in the cement extract containing 1000 ppm of chloride where the steel has undergone highest dissolution rate and the solution resistance is negligible compared to the charge transfer resistance. Under perfect passive state of the rebar, the conditions are not satisfied in all the three systems namely cement extract, mortar and concrete where solution resistance is considerably higher.
3. When the rebar embedded in cement mortar and concrete containing 3% of chloride i.e., under active state, the value of  $|Z|$  is not exactly equal to  $R_{ct}$ . It seems when the rebar undergoes either diffusion controlled reaction or charge transfer controlled reaction, the condition i.e., the value of  $Z''$  is  $< 20\%$  of  $Z'$  is only satisfied. Even then, the CR by HA is comparable to that of by EIS and weight loss method.
4. HA is relatively a rapid measurement technique with the higher degree of accuracy compared to EIS, which will vary depending on the frequency and amplitude chosen for the analysis and does not require Tafel constants for determining  $i_{\text{corr}}$ . Appropriate selection of the frequency and amplitude is necessary to differentiate the passive from active state of the rebar.

## Acknowledgements

Authors thank the Director, CECRI, Karaikudi for his kind permission to publish this paper. Authors would like to acknowledge ISARC and Centre for Corea, Korea for providing financial support.

## References

- [1] S. Feliu, J.A. González, M.C. Andrade, V. Feliu, *Corros. Sci.* 29 (1989) 105–113.
- [2] J.A. Gonzalez, A. Molina Escudero, C. Andrade, *Corros. Sci.* (1985) 917–930.
- [3] K.K. Sagoe-Crentsil, F.P. Glasser, J.T.S. Irvine, *Brit. Corros. J.* 27 (2) (1992) 113–121.
- [4] C.J. Newton, J.M. Sykes, *Corros. Sci.* 28 (11) (1988) 1051–1074.
- [5] G.K. Glass, C.L. Page, N.R. Short, J.-Z. Zhang, *Corros. Sci.* 39 (9) (1997) 1657–1662.
- [6] J.A. Gonzalez, A. Cobo, M.N. Gonzalez, S. Feliu, *Corros. Sci.* 43 (4) (2001) 611–625.
- [7] P. Garces, M.C. Andrade, A. Saez, M.C. Alonso, *Corros. Sci.* 47 (2005) 289–306.
- [8] C. Andrade, C. Alonso, J. Gulikers, *Mater. Struct.* 37 (2004) 623–643.
- [9] G.K. Glass, C.L. Page, N.R. Short, *Corros. Sci.* 32 (1991) 1283–1294.
- [10] C. Andrade, J.A. Gonzalez, *Werkst. Korros.* 29 (1978) 515–519.
- [11] J.A. Gonzalez, S. Algaba, C. Andrade, *Brit. Corros. J.* 15 (1980) 138–139.
- [12] El. Maddway, K. Soudki, *Cem. Concr. Comp.* 29 (2007) 168–175.
- [13] J. Devay, L. Meszaros, *Acta Chim. Acad. Sci. Hung.* 100 (1–4) (1979) 183–189.
- [14] S.K. Rengarajan, *J. Electroanal. Chem.* 62 (1) (1975) 31–35.
- [15] L. Meszaros, G. Meszaros, B. Lengyel, *J. Electrochem. Soc.* 141 (8) (1994) 2068–2071.
- [16] S. SathyaNarayanan, K. Balakrishnan, *Brit. Corros. J.* 29 (2) (1994) 152–155.
- [17] W. Durnie, R.D. Marco, A. Jefferson, B. Kinsella, *Corros. Sci.* 44 (2002) 1213–1221.
- [18] K. Lawson, J.D. Scantlebury, *Mater. Sci. F* 44–45 (1989) 387–392.
- [19] J.L. Dawson, D.G. John, M.I. Jafar, K. Hladky, L. Sherwood, in: C.L. Page, K.W.J. Treadway, P.B. Bamforth (Eds.), *Corrosion of Reinforcement in Concrete*, Society of Chemical Industry, USA, 1990, pp. 358–371.
- [20] S.D. Cramer, S.J. Bullard, B.S. Covino, M.Z. Moroz, G.R. Holcomb, *Intermittent application of cathodic protection – Interim report SPR (317)*, Oregon Department of Transportation Research Unit and FHWA, Washington, DC, May 2005.
- [21] K.R. Gowers, S.G. Millard, in: *ICE Proceedings Structures and Buildings*, vol. 134, no. 2, 1999, pp. 129–137.
- [22] Ha-Won Song, V. Saraswathy, *Int. J. Electrochem. Sci.* 2 (2007) 1–28.
- [23] S. Srinivasan, K. Saravanan, *Electrochemical and electrical techniques for monitoring reinforcement corrosion*, in: *Protection of Reinforcement in Concrete – An Update – Galvanizing and Other Methods*, ILZIC, New Delhi, India, 1995, pp. 33–52.
- [24] IS 8112, *Specification for 43 grade ordinary Portland cement*, BIS Standards, New Delhi, 1989.
- [25] IS 383, *Specification for coarse and fine aggregate from natural sources for concrete*, BIS standards, New Delhi, 1970.
- [26] ACI.211-91, *Standard Practise for selecting proportions for normal, heavy weight and mass concrete*, American Concrete Institute, MI, 1991.
- [27] R. Vedalakshmi, H. Dolli, N. Palaniswamy, *Struct. Control. Health Monit.* 16 (2009) 441–459.
- [28] K.C. Clear, *Transportation Research Record 1211*, Transportation Research Board 86th Annual Meeting, TSB, Washington, DC, January 1989, pp. 28–37.
- [29] J. Feils, S. Sabol, H.W. Pickering, A. Sehgal, K. Osseo-Asare, P.D. Caddy, *Corrosion* 49 (7) (1993) 601–618.
- [30] J.P. Diard, B. Le Gorec, C. Montella, *J. Electrochem. Soc.* 142 (10) (1995) 3612–3613.
- [31] V. Feliu, J.A. Gonzalez, C. Andrade, S. Feliu, *Corros. Sci.* 40 (1998) 975–993.
- [32] V. Feliu, J.A. Gonzalez, C. Andrade, S. Feliu, *Corros. Sci.* 40 (1998) 995–1001.
- [33] M. Stern, A.L. Geary, *J. Electrochem. Soc.* 104 (1975) 56–62.
- [34] ASTM G1-03, *Standard Practice for preparing, cleaning and evaluating corrosion test specimens*, ASTM Standards, vol. 03.02, 2009, pp. 9–14.
- [35] A. Pirnat, L. Meszaros, B. Lengyel, *Corros. Sci.* 37 (6) (1995) 963–973.
- [36] J. Nöggerath, H. Böhni, *Mater. Sci. F* 111–112 (1992) 659–676.
- [37] F. Pruckner, *Corrosion and Protection of Reinforcement in Concrete: Measurements and Interpretation*, Ph.D. Thesis, University of Vienna, Faculty of Natural Science and Mathematics, Vienna, 2001.
- [38] *Introduction to curve fitting* Published by National Instruments, July 2008. Available from: <<http://www.Zone.ni.com/>>.
- [39] A.J. Bard, L.R. Faulkner, *Electrochemical Methods*, Wiley, New York, 1980.